IEEE Access
Multidisciplinary | Rapid Review | Open Access Journal

Received 22 June 2023, accepted 12 August 2023, date of publication 22 August 2023, date of current version 7 September 2023.

Digital Object Identifier 10.1109/ACCESS.2023.3307436

RESEARCH ARTICLE

A Dimensional Comparative by Computed Tomography of Path Printed Fabrication Algorithms of a Multi-Geometric Piece

SINUE ONTIVEROS[1], YOLANDA BAEZ-LOPEZ[2], JULIÁN ISRAEL AGUILAR-DUQUE[2], AND JORGE LIMON-ROMERO[2]

[1]Facultad de Ciencias de la Ingeniería, Administración y Sociales, Universidad Autónoma de Baja California, Tecate 21460, Mexico
[2]Facultad de Ingeniería, Arquitectura y Diseño, Universidad Autónoma de Baja California, Ensenada 22860, Mexico

Corresponding author: Julián Israel Aguilar-Duque (julian.aguilar@uabc.edu.mx)

This work was supported by Universidad Autónoma de Baja California, Necesidades Regionales, in 2022, under Grant 402/6/C/140/7.

ABSTRACT The use and advancement of manufacturing technologies related to additive manufacturing significantly increased in the final decade of the 20th century. Technology progressions have led to the creation of methods for streamlining the printing process, emphasizing cutting down on manufacturing time, including the use of Genetic Algorithms (GA). The effect produced by changing the path pattern is interesting for two reasons: a) dimensional accuracy focused on preserving the component's dimensions and b) the structural composition and strength that the printing process itself can produce. The objective of this article is to compare the effect of modifying the path (GA) versus the manufacturer algorithm (MA) of the 3d printed in two ways, one of them focused on the accuracy dimension of the geometries and the second from the structural point of view through the comparison by using Computed Tomography. Twenty-three geometrical pieces were employed in a template printed using FFF technology and PLA as the foundation material. The total process time needed to print the component was reduced by 11% due to the findings. Regarding the dimensional analysis, the average deviation produced by the GA path is less than that produced by the manufacturer's suggestion. Regarding the porosity analysis, the GA shows a more significant void percentage but less void dispersion; ironically, the porosity concentrates based on the suggested materials. These results are crucial for product conceptualization and deposition printing planning.

INDEX TERMS Computed tomography, dimensional analysis, fused filament fabrication, impression path.

I. INTRODUCTION

A. MANUFACTURING

Innovative manufacturing techniques, global market positioning, and meeting user needs based on quality requirements are the focus of organizations to achieve development and subsistence in the market. [1], [2]. What uncertainty exists in such business development guidelines and dynamic production systems? The demand for performance indicators has concentrated on the relationship between market expansion and the rise of global powers [3]. As a result, several inflation-related economic pressures can be predicted, which will slow the expansion of the manufacturing and service sectors by 3.7% by 2025 [4], [5], [6].

The processing and service industries' growth estimates were examined, and subtractive manufacturing (SM) and additive manufacturing (AM) discovered that market development was based on technological capabilities. From one side, SM is characterized by constant flow production, homogenization of production, assembly lines, and a high degree of mechanization [7]. Conversely, AM focuses on small production runs, manufacturing complex designs and mechanisms or components requiring low mechanical [8], [9]. However, despite the clear market definitions established by SM and MA, both compete to meet the manufacturing sectors presented in Figure 1.

The associate editor coordinating the review of this manuscript and approving it for publication was Hengyong Yu.

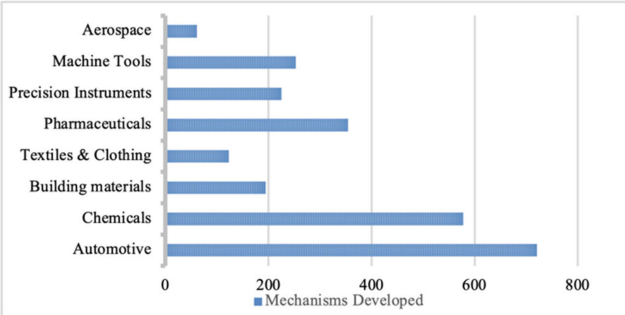

FIGURE 1. **The manufacturing industry's production areas with the fastest growth [10], [11].**

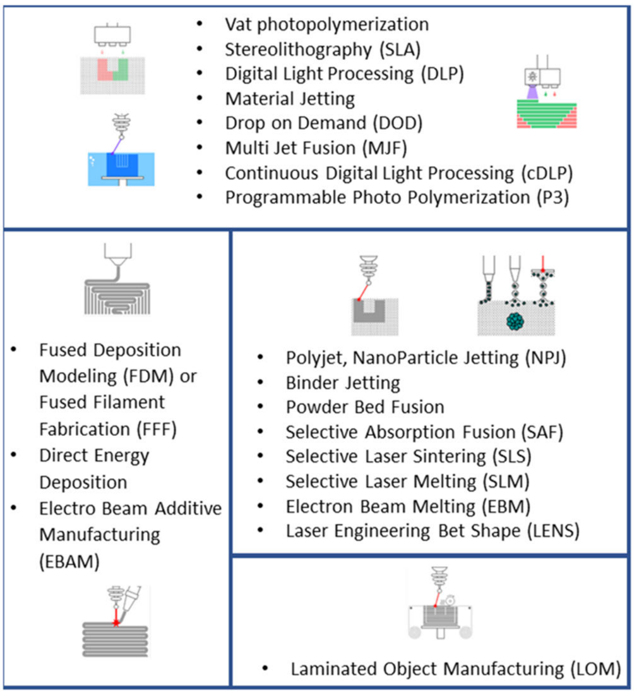

FIGURE 2. **Additive manufacturing technologies [16], [17], [18], [19].**

B. ADDITIVE MANUFACTURING

Additive manufacturing (AM), which is described as the process of layer-by-layer fabrication from a digital design [12], permeates the component manufacturing sector due to design flexibility, product customization, lower tooling costs, and, in some cases, lower costs related to logistics activities [13], [14], [15]. By 2022, 22 innovations, some of which are shown in Figure 2, will have developed from the initial AM technology patent filed in 1980.

As reported by Businesswire [10], Economics [14], Fortune [11], and Nikitakos et al. [20], in terms of the new era of manufacturing technology, additive manufacturing (AM) presents intriguing challenges centered on solving the design of complex elements to give designers design freedom. These issues should be resolved by printing in a single process, reducing or eliminating the subprocess related to quality assurance, and preserving the mechanical and functional properties that SM cannot provide.

The growth of AM has been measured at 16% for industrial production and professional services and 40% for personal use and desktop and personalized markets. It is crucial to emphasize that the reason for the growth is that the proper application of AM is linked to the reduction of material waste produced by the nature of the process, something that in the MS has required resource investment and the use of post processes.

It is important to note that, according to Makerverse [43], a v It is important to note that, according to Makerverse [21], a variety of industries are embracing AM technologies. The most important information related to the level of adoption is presented in Figure 3. For instance, only 18% of the automotive industry is using serial production for AM, compared to 52% of the medical sector.

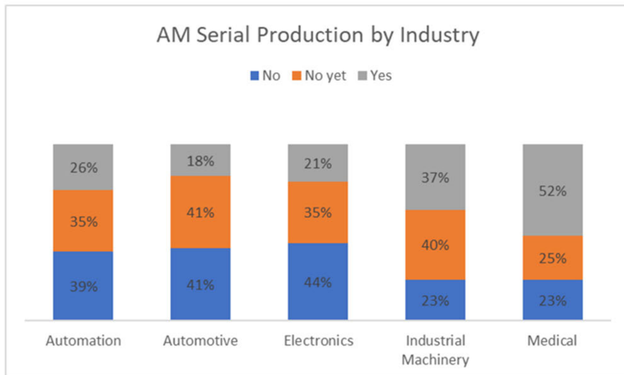

FIGURE 3. **Percentage of adopting AM Serial Production. Source [43].**

With all the advantages described above, AM has been characterized by promoting the customization of objects, thus achieving production runs of volumes as low as the unit, with constant improvements in quality and indications of repeatability in low volume products of production [22], [23], [24].

C. FUSED FILAMENT MANUFACTURING

Fused Deposition Modeling (FDM), also known as Fused Filament Fabrication (FFF), is a technique used in additive manufacturing that relies on the extrusion of thermoplastics. The printing equipment codes the component's design as the first step in the production system's layer-by-layer printing process [25].

FFF technology, which achieved a total revenue of 471.3 million, distributed in prototyping, production, proof-of-concept, market samples, art, education, and hobby applications, has emerged as the AM technology with the most significant economic gains over the past ten years, according to Market Data Forecast [26]. It is anticipated to grow at a compound annual growth rate of 18.8% over the following five years.

Despite the fact that the technology has economic advantages, FFF still has quality problems with structural deformation [27], [28], [29], dimensional deformation [30], [31], low quality [32], [33], [34], and processing time [35], [36], which makes it challenging to use this technology for the direct digital fabrication of objects.

D. OPTIMIZATION ALGORITHM

One strategy adopted by software developers of printing equipment aimed at reducing the dimensional defects and surface polish generated by the FFF process was the implementation and creation of various programming algorithms. Based on the outcomes of their application in computer numerical control (CNC) machinery, these algorithms were created. Robot path optimization for machining [37], Genetic Algorithm (GA) for reducing tool travel time without increasing the component's value (tool air time) [38], GA for reducing operating time and operating parameter variation [39], [40], and most recently Yodo and Dey [41] presented their idea for multi-objective optimization based on evolutionary algorithms.

As was already said, there has been a tremendous advancement in the use of GAs to optimize CNC or extrusion tool paths. It is important to highlight that hybrid approaches have also been employed to shorten processing times, in addition to those for artificial immune systems (AIS) and artificial neural networks (ANN) [42], GA with Particle Swarm Optimization (PSO) [43], or that of Ülker et al. [44]. Examples include combining a parameter-focused Neural Networks Algorithm (ANN) with a response surface algorithm [45] or combining hybrid particle swarming with bacterial foraging optimization to improve operating parameters [46].

GAs have been explicitly included in the FFF to improve the performance of this technology based on the operational parameters and the computation of their optimal operating values [13], [36], as demonstrated by [47] with the parameter optimization model.

The FFF method is without a doubt an alternative for the creation of 3D printed components, but there is room for improvement from a variety of research perspectives due to the length of time needed for component manufacturing and dimensional finishing. It is possible to use routing models in accordance with the principles of transport techniques, in which the tool's (the extruder) path is determined by the responses to two questions: the first asks about the curve to be traced, and the second asks about the direction in which the curve will be printed. The mathematical expression of this concept for decision-making is shown as a function of two variables:

$$\begin{aligned} X_i &= \{1 \; \textit{if the initial vertex of arc } i \textit{ is } v_{i1} \; 0 \\ &\qquad \textit{if the inictial vertex of arc } i \textit{ is } v_{i2} \\ Y_{ij} &= \{1 \; \textit{if the } i-th \textit{ traced arc } arc_j \; 0 \textit{ any other case} \end{aligned} \tag{1}$$

The target function of the model using the aforementioned variables is to minimize the total run time, namely the air time, which has no bearing on the component print. The time required varies with the distance traveled between subsequent arcs according to the following function:

$$\begin{aligned} MinZ = &\sum_{j=1}^{n} Y_{1j}\left[X_j a_{0j} + \left(1 - X_j\right) a_{1j}\right] \\ &+ \sum_{j=1}^{n} Y_{nj}\left[X_j a_{1j} + \left(1 - X_j\right) a_{0j}\right] \\ &+ \sum_{i=1}^{n-1}\sum_{j=1}^{n} Y_{ij}\left(\sum_{i=1}^{n} Y_{i+1,l} Z_{jl}\right) \end{aligned} \tag{2}$$

where

$$\begin{aligned} Z_{jl} = &X_j X_l a_{jl} + X_j\left(1 - X_l\right) b_{jl} + \left(1 - X_j\right) X_l c_{jl} \\ &+ \left(1 - X_j\right)\left(1 - X_l\right) d_{jl} \end{aligned}$$

n is the total number of curves to be printed.

$$\begin{aligned} a_{ij} &= distance\left(v_{i2}, v_{j1}\right) \\ b_{ij} &= distance\left(v_{i2}, v_{j2}\right) \\ c_{ij} &= distance\left(v_{i1}, v_{j1}\right) \\ d_{ij} &= distance\left(v_{i1}, v_{j1}\right) \\ a_{0j} &= distance\left(origin, v_{j1}\right) \\ a_{1j} &= distance\left(origin, v_{j2}\right) \end{aligned}$$

With Tuker's formulation, the transport model can have the following objective function thanks to the inclusion of constraints that prevent loops:

$$MinZ = \sum_{i=1}^{n}\sum_{j=1}^{n} Y_{ij} D_{ij} \tag{3}$$

subject to:

$$\begin{aligned} &\sum_{j=1}^{n} Y_{ij} = 1 \; for \; i = 1 \; until \; n, \\ &\sum_{i=1}^{n} Y_{ij} = 1 \; for \; j = 1 \; until \; n, \\ &Y_{ij} = [0, 1] \\ &u_i - u_j + p y_{ij} \leq p - 1 para \; i = 1, \ldots n; j = 1, \ldots, n; i \neq j \end{aligned}$$

The objective function of the prior model, where u_i are variables, represents p as the maximum number of nodes the extruder must pass over from its starting point until it has finished printing the layer. The integer programming model principle is used to determine the best order for viewing the arcs.

E. COMPUTED TOMOGRAPHY

It is no secret that Computed Tomography (CT) has developed into an essential instrument for the study and development of production processes, principally because it can do many analyses and provides quicker access to a part's interior than conventional measuring methods [48], [49]. Without having to separate the workpiece in order to perform reverse engineering, it is possible to create a 3D model of the workpiece and perform internal analyses of the part (even in regions that are not visible to the eye), dimensional analysis, and analyses of multi-material parts using just one scanner. Simulated operations can be carried out using the 3D representation of the workpiece without affecting or damaging the component [50].

CT is widely employed in additive manufacturing processes and to examine complex geometry. The two most important quality control analyses for these parts are part interior analysis and dimensional correctness. Khosravany and Reinicke [51] presented a summary of commercial and scholarly applications and models produced using various additive manufacturing processes or techniques in various materials and shapes, all with regular geometries or repeatable manufacturing patterns, all to analyze porosity and material density. On the other hand, Cho and Lee [52] demonstrated the use of CT for the investigation of material density and porosity in a dog-bone-shaped specimen produced in carbon fiber reinforced plastic.

In the study by Tkac et al. [53], a part's porosity is examined using CT, using a 3D-printed replica of the lattice structure as a base. The mechanical structural study in [54] uses the same component. The portions stated in the previous paragraphs have one thing in common: they all have simple or recurring geometries. The current study aims to evaluate the structural quality and dimensional finish of a component composed of numerous geometric parts.

II. METHODOLOGY

Figure 4 shows the flowchart of the methodology used.

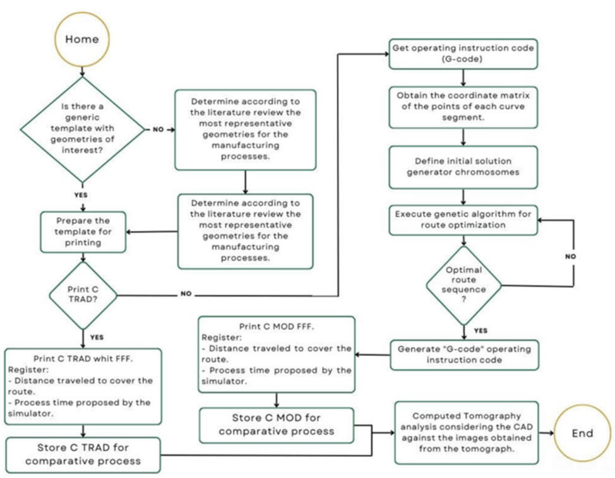

FIGURE 4. Flowchart of the methodology.

The following steps were taken in the development of the current study:

A. MULTI-GEOMETRIC COMPONENT

Using the Aguilar-Duque et al. [55] model. The adjustments involved rearranging the geometric pieces and incorporating two threaded cylindrical components.

B. MULTI-GEOMETRIC COMPONENT'S PREPROCESSING

The printer was set up, taking into account the characteristics mentioned in Table 1 to calculate the processing time required to print the proposed template.

TABLE 1. FFF printing equipment operating parameters [1].

	Magnitude	Reference
Nozzle diameter	0.300 mm	[56]
Layer height	0.150 mm	[57, 58]
Wall thickness	0.800 mm	[58, 59]
Upper/lower thickness	0.800 mm	
Filling density	100%	[16, 60]
Filling pattern	Lines	
Material Printing temperature	215°C	[61, 62]
Printing bed temperature	60°C	
Filament Diameter	1.750 mm	
Flow	100%	
Retraction	Enabled	
Printing speed	60 mm/s	[16, 58]
Travel speed	120 mm/s	
Print cooling	Activate	[63]
Generate support	Active for -Z	[64-67]
Support placement	Everywhere	
Type of adhesion	Border	[56, 64, 65, 68]
Edge width	8.000 mm	

C. PREPROCESSING OF THE MULTI-GEOMETRIC COMPONENT

The control template and the template with the GA modified route technique were manufactured using an Ultimaker S5 printer. The printing equipment was set up in accordance with the specifications provided in Table 2 after taking into account the recommendations for the parameters found in the literature review.

TABLE 2. Printing equipment characteristics.

Feature	Technical data
Print size	330 x 240 x 300 mm
Feeding	100 – 240 VAC, 50 – 60 Hz
Software	Ultimaker Cura
XYZ Resolution	6.9, 6.9, 2.5 µ
Nozzle diameter	0.25
Nozzle temperature	180 – 260 ºC
Bed temperature	20 – 110 ºC
Printing speed	<24 mm3/s

Polylactic acid filament (PLA) has been used for printing. Table 3 presents the characteristics of the substance as stated in the manufacturer's data sheet. Table 4 presents the characteristics of the substance as stated in the manufacturer's data sheet.

TABLE 3. **PLA characteristics.**

Characteristic	Specification
Appearance	Filament
Color	White
Ignition temperature	388 ºC
Thermal decomposition	250 ºC
Melting point/melting range	145 – 160 ºC
Density	1.240 g/cm3

To prepare the materials for the process, they were kept in an air-conditioned space between 23 and 25 °C for at least 40 hours. This was done while the printing equipment was being set up.

After printing, vacuum packaging with insulation was employed to keep the components' dimensions unchanged and to guard against size changes, shocks, and temperature fluctuations. The components were kept and subjected to an air-conditioning process inside a room with temperature and humidity control for at least 40 hours at a temperature of 20 + 2°C and a relative humidity without condensation of 50 + 10% in preparation for the digitization process. The component was scanned using the ZEISS Metrotom 800 CT scanner, which provides highly accurate measurements of plastic parts.

D. MEASUREMENT OF COMPONENTS

The dimension analysis of the multi geometric templates was measured using Geomagic, and VG Studio was used for porosity analysis. The geometric shapes were constructed using a point cloud of the workpiece, constantly avoiding the edges of the parts to prevent influence from potential flaws. According to the reference coordinates, each component was measured. The comparative study takes into account the relevant characteristics listed in Table 4.

TABLE 4. **Components attributes.**

Feature	Geometry
Base	Base, set of blocks, pyramid overhang
Prisms	Base quadrangular groove, perforated cube, ladder, grooves.
Cylindrical drilling	Coaxial cylinders, base pass-through drilling, base drilling, cube-drills
Sphere	Set of spheres
Solid cylinder	Concave semi-cylinders
Hollow cylinder	Convex semi-cylinders, cantilevered arch.
Cone	Truncated cones
Angled surfaces	Truncated cones, triangular perforation, staircase, inclined planes, pyramid of blocks

The multi geometric template has some geometric components on the lateral face and 23 geometric components in the upper section. 134 attributes are considered for the analysis. Figure 5 presents a CAD of the multi-geometric template component.

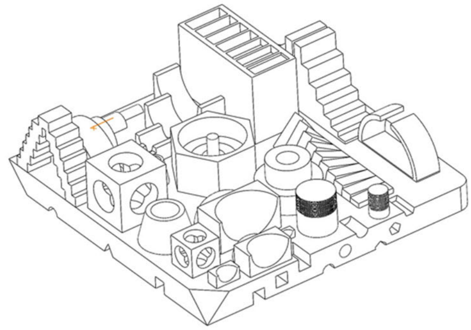

FIGURE 5. **Multi-geometric template.**

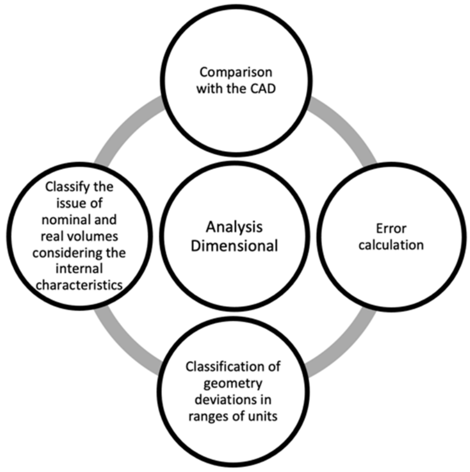

FIGURE 6. **Comparison of nominal versus actual CAD.**

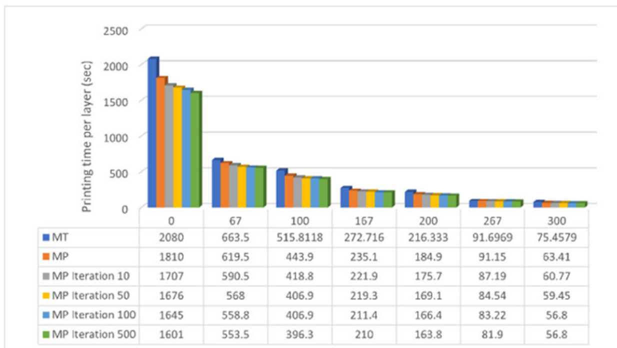

FIGURE 7. **Manufacturing time.**

E. COMPARISON OF NOMINAL VERSUS ACTUAL CAD

The inaccuracy produced by the printing process is identified by tomographic analysis using the dimensions supplied in the design, according to the following diagram (Figure 6):

III. RESULTS

A. REDUCTION OF MANUFACTURING TIME THROUGH GA

According to the preprocess of the manufacturer, 25.03 hours are required to print the component, using 14.34 meters of

PLA. When comparing the manufacturing time suggested by the manufacturer's preprocess program to the route modification generated by the GA, the tool path change results in a decrease of 11%. Figure 7 presents the comparative time generated by the de-manufacturer (MT) versus the modified process (MP) of 7 layers considering the original route, 10 iterations, 50 iterations, 100 iterations, and 500 iterations of the algorithm optimizing the printing time. The selection of the layers for the representation of the graph was performed randomly.

B. DIMENSIONAL ANALYSIS

In order to make a first comparison and obtain a global reference for the quality of the pieces, a CAD comparison has been made. Table 5 summarizes the data obtained; the maximum deviation of the Genetic Algorithm (GA) is less than that of the Manufacturer (MA), and the minimum deviation is very similar. The average positive and negative deviation of the genetic algorithm is also lower than that of the Manufacturer, and the standard deviation is also lower, being 0.191 mm for GA and 0.323 for MA. The standard deviation is lower as well, at 0.191 mm for GA and 0.323 for MA.

TABLE 5. CAD comparison results.

Information	Genetic Algorithm (GA)	Manufacturer Algorithm (MA)
Max	+5.573	+5.731
Min	-5.774	-5.733
Average deviation	+0.147	+0.154
positive	-0.124	-0.187
Average deviation	0.194	0.323

Figure 8 shows images of the CAD comparison; it is possible to see that the minimum deviation is in the exact area of the figure in both cases, whereas the maximum deviation is in a different area of the figures. In addition to the green color of both (which indicates little deviation), the light blue color predominates in the GA piece, which indicates that the deviation is negative in those areas. In the MA piece, the yellow color predominates, meaning the deviation in that area is positive.

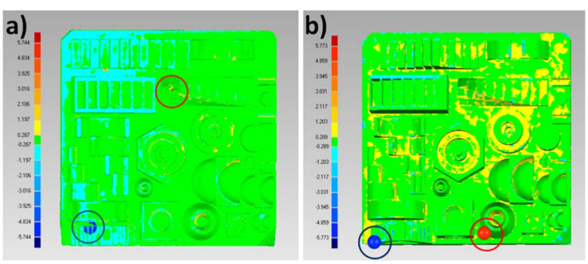

FIGURE 8. CAD deviation. a) Genetic algorithm path and b) Manufacturer algorithm path CAD comparison.

Figure 9 compares the maximum positive deviation of the GA part and the same area of the MA part; remarkably, the finishes of the printed elements are deficient in the angled elements and irregular in the planes in both cases.

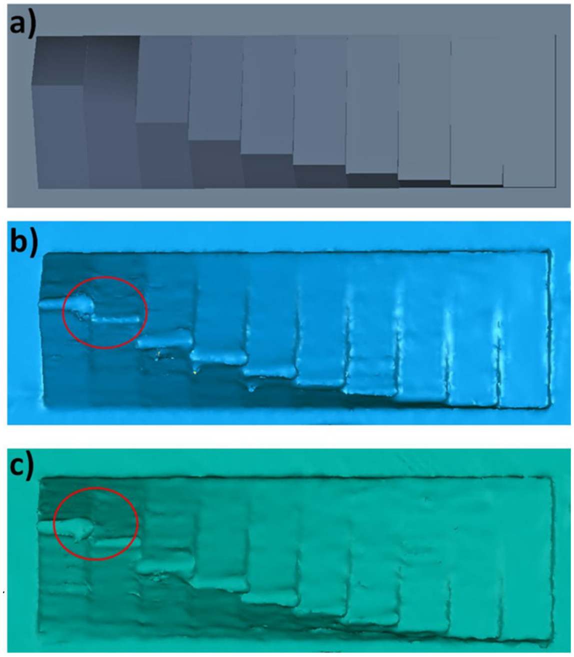

FIGURE 9. Comparison of maximum positive deviation point, a) CAD, b) GA piece y c) MA piece.

Figure 10 circles the maximum negative deviation and its comparison through the CAD; the figure exposes a significant quality defect, including extra elements to the original component in both cases and similar areas of the same piece.

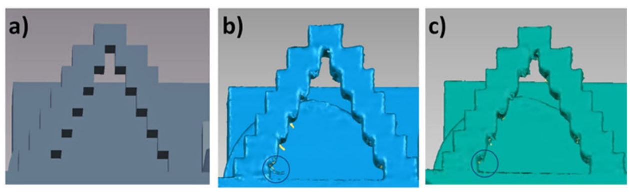

FIGURE 10. Comparison of maximum negative deviation point, a) CAD, b) GA piece y c) MA piece.

With the purpose of carrying out a detailed comparison by type of component, three groups have been generated: lengths, angles, and diameters. Figure 11 shows the absolute lengths deviations of the 3D volume measurement generated with CT from the original CAD design; blue bars describe the deviations from GA, green bars are from MA, and the red line is the tolerance. The average deviation for the GA is smaller than MA, being 0.159 mm and 0.253 mm, respectively; the maximum deviation is higher for MA, and the minimum and standard deviation are similar in both cases, around 0.010 mm and 0.170 mm, respectively. It is also possible to observe that in the GA part, two lengths are out of tolerance while three are out of tolerance for the MA piece.

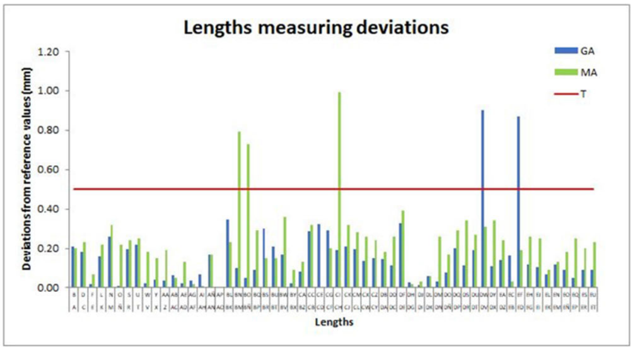

FIGURE 11. Measurement deviation (absolute values) lengths.

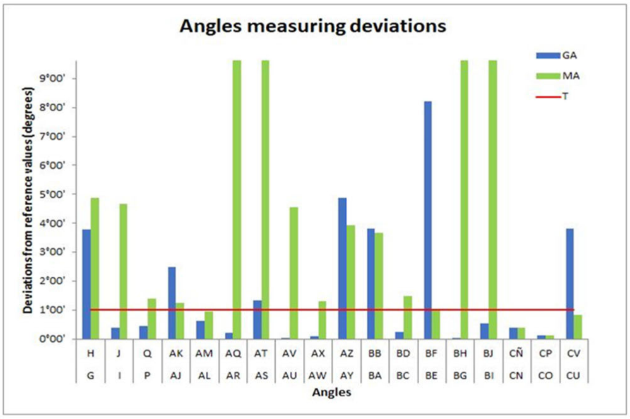

FIGURE 12. Measurement deviation (absolute values) angles.

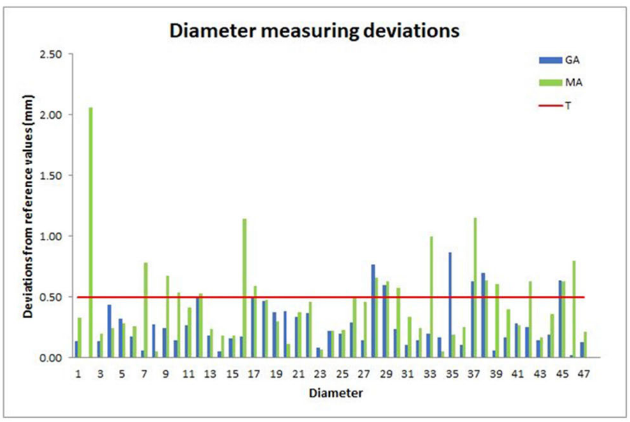

FIGURE 13. Measurement deviation (absolute values) diameters.

Figure 12 presents the absolute angle measurement deviations of both pieces. It is possible to highlight that 9 out of 22 evaluated attributes are out of tolerance for the GA piece for 13 for the MA piece, the average deviation is 1°44' and 5°34' for GA and MA, respectively, and the maximum value and the standard deviation is smaller for the GA.

Figure 13 exposes the absolute deviation of the measurement of diameters. The average deviation is 0.277 mm, whit a maximum value of 0.870 mm and a minimum value of

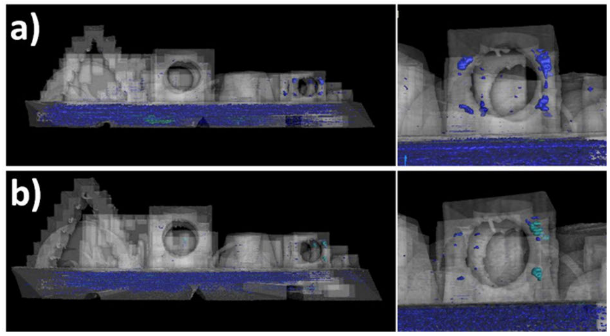

FIGURE 14. Lateral views of the work pieces, a) GA piece and b) MA piece.

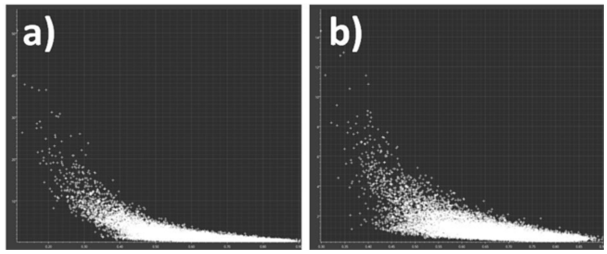

FIGURE 15. Distribution of porosity spheres.

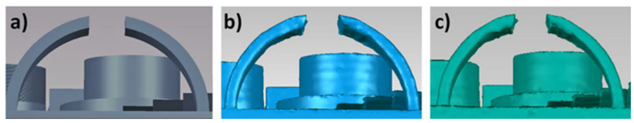

FIGURE 16. Comparison of defect of the cantilevered arc geometry, a) CAD, b) GA piece and c) MA piece.

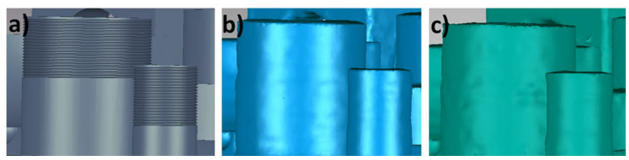

FIGURE 17. Comparison of threaded element defects, a) CAD, b) GA piece and c) MA piece.

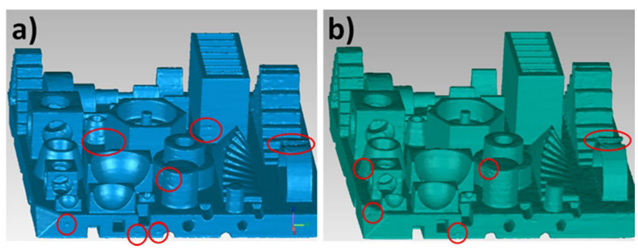

FIGURE 18. Elements with quality defects.

0.006 mm for the GA piece. In comparison, the average deviation is 0.461 mm, with 2.016 mm as a maximum value and 0.051 mm as a minimum value for the MA piece. In the three comparisons, the best results are for the GA piece.

Six diameters are out of tolerance for GA, while 17 are out for MA.

C. STRUCTURAL ANALYSIS

Component infill in AM is a key parameter affecting porosity and print time, so porosity analysis is essential to determine manufacturing system capability. In this study, the GA piece has around 2% porosity, and the MA piece is around 0.5% porosity of the total volume. Figure 14 shows that most of the porosity is at the base of both pieces, and the geometry with greater porosity in both cases is the same.

Figure 15 shows the distribution of porosity spheres or holes. Figure 15a depicts the distribution of part GA, and Figure 15b depicts part MA. Although the percentage of porosity is better in AM, a more excellent dispersion of porosity can be observed.

Another relevant aspect in AM is the surface finish and layer resolution. Two figures present problems in defining the characteristics of the geometries regardless of the algorithm used. Figure 16 exposes a quality problem in the planes of the cantilevered arch in both pieces.

In Figure 17, something similar happens to the previous geometry; the 3D printer cannot print geometries of threaded elements.

Figure 18 presents an isometric view of the workpieces. Printing defects on the external faces of the geometries are highlighted in red circles. Some of the zones are coincident in both pieces.

IV. CONCLUSION

Production systems have focused their efforts on the optimization of operational and administrative resources. With the implementation of AG in this project, it was possible to reduce the production time of the component by 11%. However, the time required to prepare the process can compensate for this saving; the benefits obtained by it are achieved by having an optimal production program that ensures a shorter production time than estimated by default.

The results based on tomographic analysis show a coincidence in terms of the minimum dimensional deviation concerning the two components (control template and modified template). Concerning the printing of the components, it is clear that the GA template presents negative dimensional deviations in quadrangular base elements specifically, compared to the positive deviations identified in the angular and cylindrical elements generated by the process proposed by the manufacturer. As for the dimensional accuracy of the components, the AG has on average more minor deviations than those generated by the manufacturer's proposal.

As for the porosity analysis, the GA presents a higher percentage in terms of porosity, which coincidentally focuses based on the proposed elements. It is also possible to identify that the cylindrical elements present a greater degree of complexity during the printing process that forces the process to generate porosity due to the stepped deposit of the material. It is worth mentioning that although the percentage of porosity in the MA is lower, the dispersion of the same is more remarkable, thereby identifying a process with lower porosity. However, with more excellent dispersion or degree of error, this is an advantage for the AG that despite having greater porosity, this has less variability than the MA.

Finally, these findings are essential for the conceptualization of products and the planning of deposition printing processes in which customized elements require a shorter response time, such as those required in the medical industry with the replication of orthoses and prostheses, those of the aerospace industry from the maintenance approach in even those required by the military industry that requires precision and resistance.

REFERENCES

[1] B. Kajwang, "Global challenges and their role in talent management crisis facing insurance industry," *Int. J. Bus. Strategies*, vol. 7, no. 1, pp. 1–10, Jan. 2022.

[2] M. Kehayov, L. Holder, and V. Koch, "Application of artificial intelligence technology in the manufacturing process and purchasing and supply management," *Proc. Comput. Sci.*, vol. 200, pp. 1209–1217, Jan. 2022.

[3] *Global Manufacturing Output Growth Reaches 3.9 for 2022*. Accessed: Jun. 12, 2022. [Online]. Available: https://www.automation.com/en-us/articles/september-2022/global-manufacturing-output-growth-2022

[4] A. A. A. O'Gli, "Principles of financial innovation," Tech. Rep., 2022.

[5] P. Gazzola, E. Pavione, R. Pezzetti, and D. Grechi, "Trends in the fashion industry. The perception of sustainability and circular economy: A gender/generation quantitative approach," *Sustainability*, vol. 12, no. 7, p. 2809, Apr. 2020.

[6] F. Omonov and Q. Dehqonov, "Electric cars as the cars of the future," *Eurasian J., Eng. Sci. Technol.*, vol. 4, pp. 128–133, Jan. 2022.

[7] S. Kalpakjian and S. R. Schmid, *Manufacturing, Engineering and Technology*, 7th ed. New Jersey, NJ, USA: Pearson, 2014.

[8] Mordor Intellingence. *Additive Manufacturing & Materials Market—Growth, Trends, and Forecast (2020–2025)*. Accessed: Apr. 13, 2020. [Online]. Available: https://www.mordorintelligence.com/industry-reports/global-additive-manufacturing-and-material-market-industry

[9] H. C. Sonar, V. Khanzode, and M. Akarte, "A conceptual framework on implementing additive manufacturing technology towards firm competitiveness," *Int. J. Global Bus. Competitiveness*, vol. 15, no. 2, pp. 121–135, Dec. 2020.

[10] Businesswire. *Global Smart Factory Market Research Report 2022–2027: Analysis of SCADA, PM, MES, Industrial Safety, Industrial Sensors, Industrial Robots, Industrial 3D Printers, Machine Vision Systems*. Accessed: Jun. 12, 2022. [Online]. Available: https://www.businesswire.com/news/home/20221205005517/en/Global-Smart-Factory-Market-Research-Report-2022-2027-Analysis-of-SCADA-PAM-MES-Industrial-Safety-Industrial-Sensors-Industrial-Robots-Industrial-3D-Printers-Machine-Vision-Systems—ResearchAndMarkets.com

[11] F. B. Insights. *E Global 3D Printing Market is Projected to Grow From $18.33 Billion in 2022 to $83.90 Billion by 2029, at a CAGR of 24.3% in Forecast Period, 2022-20289*. Global Research Report. Accessed: May 5, 2023. [Online]. Available: http://www.fortunebusinessinsights.com

[12] *Standard Terminology for Additive Manufacturing—Coordinate Systems and Test Methodologies*, A. I. S. Organization, 2013.

[13] S. Deswal, R. Narang, and D. Chhabra, "Modeling and parametric optimization of FDM 3D printing process using hybrid techniques for enhancing dimensional preciseness," *Int. J. Interact. Design Manuf.*, vol. 13, no. 3, pp. 1197–1214, Sep. 2019, doi: 10.1007/s12008-019-00536-z.

[14] Oxford Economics. (2019). *The Future of Global Manufacturing*. Oxford, U.K. [Online]. Available: https://www.oxfordeconomics.com/

[15] M. Tanenbaum and W. Holstein. *Mass Production*. Accessed: Apr. 15, 2019. [Online]. Available: https://www.britannica.com/technology/mass-production

[16] T. S. Srivatsan and T. S. Sudarchan, *Additive Manufacturing. Innovations, Advances, and Applications*, 1st ed. Boca Raton, FL, USA: Taylor & Francis, 2016, p. 444.

[17] D. Bourell, J. J. Beaman, H. L. Marcurs, and J. W. Barlow, ‘‘Solid Freform fabrication an advanced manufacturing approach,’’ in *Proc. Int. Solid Freeform Fabr. Symp.*, 1990, p. 7, doi: 10.15781/T2W08X029.

[18] I. Campbell, D. Bourell, and I. Gibson, ‘‘Additive manufacturing: Rapid prototyping comes of age,’’ *Rapid Prototyping J.*, vol. 18, no. 4, pp. 255–258, Jun. 2012, doi: 10.1108/13552541211231563.

[19] *Standard Terminology for Additive Manufacturing Technologies*, Standard F2792, Geneva, Switzerland, 2013.

[20] N. Nikitakos, I. Dagkinis, D. Papachristos, G. Georgantis, and E. Kostidi, ‘‘Economics in 3D printing,’’ in *3D Printing: Applications in Medicine and Surgery*. Amsterdam, The Netherlands: Elsevier, 2020, ch. 6, pp. 85–95.

[21] Makerverse. *WhitePaper: The Biggest Additive Manufacturing Trends of 2023*. Accessed: May 5, 2023. [Online]. Available: http://www.makerverse.ai

[22] Y. AbouelNour and N. Gupta, ‘‘In-situ monitoring of sub-surface and internal defects in additive manufacturing: A review,’’ *Mater. Des.*, vol. 222, Oct. 2022, Art. no. 111063.

[23] M. Brennan, J. Keist, and T. Palmer, ‘‘Defects in metal additive manufacturing processes,’’ *J. Mater. Eng. Perform.*, vol. 30, no. 7, pp. 4808–4818, 2021.

[24] B. Wu, Z. Pan, D. Ding, D. Cuiuri, H. Li, J. Xu, and J. Norrish, ‘‘A review of the wire arc additive manufacturing of metals: Properties, defects and quality improvement,’’ *J. Manuf. Processes*, vol. 35, pp. 127–139, Oct. 2018.

[25] S. S. Crump, ‘‘Apparatus and method for creating three-dimensional objects,’’ Patent U.S. 5 121 329 A, Jun. 1992. [Online]. Available: https://patents.google.com/patent/US5121329A/en?oq=5121329

[26] M. D. Forecast. *3D Printing Market*. Accessed: Dec. 12, 2022. [Online]. Available: http://www.marketdataforecast.com

[27] K. Singh, ‘‘Experimental study to prevent the warping of 3D models in fused deposition modeling,’’ *Int. J. Plastics Technol.*, vol. 22, no. 1, pp. 177–184, Jun. 2018.

[28] J. Xie, A. Saluja, A. Rahimizadeh, and K. Fayazbakhsh, ‘‘Development of automated feature extraction and convolutional neural network optimization for real-time warping monitoring in 3D printing,’’ *Int. J. Comput. Integr. Manuf.*, vol. 2022, pp. 1–18, Jan. 2022.

[29] K. Paraskevoudis, P. Karayannis, and E. P. Koumoulos, ‘‘Real-time 3D printing remote defect detection (stringing) with computer vision and artificial intelligence,’’ *Processes*, vol. 8, no. 11, p. 1464, Nov. 2020.

[30] J. Liao, Z. Shen, G. Xiong, C. Liu, C. Luo, and J. Lu, ‘‘Preliminary study on fault diagnosis and intelligent learning of fused deposition modeling (FDM) 3D printer,’’ in *Proc. 14th IEEE Conf. Ind. Electron. Appl. (ICIEA)*, Jun. 2019, pp. 2098–2102.

[31] A. Milovanović, M. Milošević, G. Mladenović, B. Likozar, K. Čolić, and N. Mitrović, ‘‘Experimental dimensional accuracy analysis of reformer prototype model produced by FDM and SLA 3D printing technology,’’ in *Experimental and Numerical Investigations in Materials Science and Engineering*. Cham, Switzerland: Springer, 2018, pp. 84–95.

[32] R. S. Zagidullin, N. I. Zezin, and N. V. Rodionov, ‘‘Improving the quality of FDM 3D printing of UAV and aircraft parts and assemblies by parametric software changes,’’ *IOP Conf. Ser., Mater. Sci. Eng.*, vol. 1027, no. 1, Jan. 2021, Art. no. 012031.

[33] P. Ferretti, C. Leon-Cardenas, G. M. Santi, M. Sali, E. Ciotti, L. Frizziero, G. Donnici, and A. Liverani, ‘‘Relationship between FDM 3D printing parameters study: Parameter optimization for lower defects,’’ *Polymers*, vol. 13, no. 13, p. 2190, Jun. 2021.

[34] S. Wickramasinghe, T. Do, and P. Tran, ‘‘FDM-based 3D printing of polymer and associated composite: A review on mechanical properties, defects and treatments,’’ *Polymers*, vol. 12, no. 7, p. 1529, Jul. 2020.

[35] A. Dey and N. Yodo, ‘‘A systematic survey of FDM process parameter optimization and their influence on part characteristics,’’ *J. Manuf. Mater. Process.*, vol. 3, no. 3, p. 64, Jul. 2019.

[36] A. Jaisingh Sheoran and H. Kumar, ‘‘Fused deposition modeling process parameters optimization and effect on mechanical properties and part quality: Review and reflection on present research,’’ *Mater. Today, Proc.*, vol. 21, pp. 1659–1672, Jan. 2020.

[37] C.-J. Chen and C.-S. Tseng, ‘‘The path and location planning of workpieces by genetic algorithms,’’ *J. Intell. Manuf.*, vol. 7, no. 1, pp. 69–76, Feb. 1996, doi: 10.1007/BF00114139.

[38] K. Castelino, R. D’Souza, and P. K. Wright, ‘‘Toolpath optimization for minimizing airtime during machining,’’ *J. Manuf. Syst.*, vol. 22, no. 3, pp. 173–180, 2003, doi: 10.1016/S0278-6125(03)90018-5.

[39] R. K. Agrawal, D. K. Pratihar, and A. R. Choudhury, ‘‘Optimization of CNC isoscallop free form surface machining using a genetic algorithm,’’ *Int. J. Mach. Tools Manuf.*, vol. 46, nos. 7–8, pp. 811–819, Jun. 2006, doi: 10.1016/j.ijmachtools.2005.07.028.

[40] P. Palanisamy, I. Rajendran, and S. Shanmugasundaram, ‘‘Optimization of machining parameters using genetic algorithm and experimental validation for end-milling operations,’’ *Int. J. Adv. Manuf. Technol.*, vol. 32, nos. 7–8, pp. 644–655, Mar. 2007, doi: 10.1007/s00170-005-0384-3.

[41] N. Yodo and A. Dey, ‘‘Multi-objective optimization for FDM process parameters with evolutionary algorithms,’’ in *Fused Deposition Modeling Based 3D Printing*, 2021, pp. 419–444.

[42] F. Cus, J. Balic, and U. Zuperl, ‘‘Hybrid ANFIS-ants system based optimisation of turning parameters,’’ *J. Achiev. Mater. Manuf. Eng.*, vol. 36, no. 1, pp. 79–86, 2009.

[43] C. Oysu and Z. Bingul, ‘‘Tool path optimization using genetic algorithms,’’ in *Proc. GEM*, 2007, pp. 120–126.

[44] E. Ülker, M. E. Turanalp, and H. S. Halkaci, ‘‘An artificial immune system approach to CNC tool path generation,’’ *J. Intell. Manuf.*, vol. 20, no. 1, pp. 67–77, Feb. 2009, doi: 10.1007/s10845-008-0104-6.

[45] S. Deshwal, A. Kumar, and D. Chhabra, ‘‘Exercising hybrid statistical tools GA-RSM, GA-ANN and GA-ANFIS to optimize FDM process parameters for tensile strength improvement,’’ *CIRP J. Manuf. Sci. Technol.*, vol. 31, pp. 189–199, Nov. 2020.

[46] M. Raju, M. K. Gupta, N. Bhanot, and V. S. Sharma, ‘‘A hybrid PSO–BFO evolutionary algorithm for optimization of fused deposition modelling process parameters,’’ *J. Intell. Manuf.*, vol. 30, no. 7, pp. 2743–2758, Oct. 2019.

[47] V. H. Nguyen, T. N. Huynh, T. P. Nguyen, and T. T. Tran, ‘‘Single and multi-objective optimization of processing parameters for fused deposition modeling in 3D printing technology,’’ *Int. J. Automot. Mech. Eng.*, vol. 17, no. 1, pp. 7542–7551, Mar. 2020, doi: 10.15282/ijame.17.1.2020.03.0558.

[48] S. Ontiveros, R. Jiménez, J. Yagüe-Fabra, and M. Torralba, ‘‘Analysis of surface extraction methods based on gradient operators for computed tomography in metrology applications,’’ *Materials*, vol. 11, no. 8, p. 1461, Aug. 2018, doi: 10.3390/ma11081461.

[49] H. Villarraga-Gómez, C. Lee, and S. T. Smith, ‘‘Dimensional metrology with X-ray CT: A comparison with CMM measurements on internal features and compliant structures,’’ *Precis. Eng.*, vol. 51, pp. 291–307, Jan. 2018, doi: 10.1016/j.precisioneng.2017.08.021.

[50] L. De Chiffre, S. Carmignato, J.-P. Kruth, R. Schmitt, and A. Weckenmann, ‘‘Industrial applications of computed tomography,’’ *CIRP Ann.*, vol. 63, no. 2, pp. 655–677, 2014, doi: 10.1016/j.cirp.2014.05.011.

[51] M. R. Khosravani and T. Reinicke, ‘‘On the use of X-ray computed tomography in assessment of 3D-printed components,’’ *J. Nondestruct. Eval.*, vol. 39, no. 4, p. 75, Dec. 2020, doi: 10.1007/s10921-020-00721-1.

[52] S.-Y. Cho and J.-R. Lee, ‘‘Investigation of manufacturing defects in 3D-printed CFRP using laser ultrasonic testing and X-ray micro-computed tomography,’’ *Funct. Compos. Struct.*, vol. 3, no. 2, Jun. 2021, Art. no. 025005, doi: 10.1088/2631-6331/ac034d.

[53] J. Tkac, T. Toth, V. Molnar, M. Dovica, and G. Fedorko, ‘‘Possibilities of analysis of porous structures using industrial computed tomography,’’ *Eng. Failure Anal.*, vol. 137, Jul. 2022, Art. no. 106296, doi: 10.1016/j.engfailanal.2022.106296.

[54] J. Tkac, T. Toth, V. Molnar, M. Dovica, and G. Fedorko, ‘‘Observation of porous structure’s deformation wear after axial loading with the use of industrial computed tomography (CT),’’ *Measurement*, vol. 200, Aug. 2022, Art. no. 111631, doi: 10.1016/j.measurement.2022.111631.

[55] J. I. Aguilar-Duque, C. O. Balderrama-Armendáriz, C. A. Puente-Montejano, A. S. Ontiveros-Zepeda, and J. L. García-Alcaraz, ‘‘Genetic algorithm for the reduction printing time and dimensional precision improvement on 3D components printed by fused filament fabrication,’’ *Int. J. Adv. Manuf. Technol.*, vol. 115, nos. 11–12, pp. 3965–3981, Aug. 2021.

[56] I. J. Solomon, P. Sevvel, and J. Gunasekaran, ‘‘A review on the various processing parameters in FDM,’’ *Mater. Today, Proc.*, vol. 37, pp. 509–514, Jan. 2021.

[57] D. Ahn, H. Kim, and S. Lee, ‘‘Fabrication direction optimization to minimize post-machining in layered manufacturing,’’ *Int. J. Mach. Tools Manuf.*, vol. 47, nos. 3–4, pp. 593–606, Mar. 2007, doi: 10.1016/j.ijmachtools.2006.05.004.

[58] O. A. Mohamed, S. H. Masood, and J. L. Bhowmik, "Optimization of fused deposition modeling process parameters: A review of current research and future prospects," *Adv. Manuf.*, vol. 3, no. 1, pp. 42–53, Mar. 2015, doi: 10.1007/s40436-014-0097-7.

[59] A. K. Sood, R. K. Ohdar, and S. S. Mahapatra, "Improving dimensional accuracy of fused deposition modelling processed part using grey Taguchi method," *Mater. Des.*, vol. 30, no. 10, pp. 4243–4252, Dec. 2009, doi: 10.1016/j.matdes.2009.04.030.

[60] P. R. Srivastava, "A cooperative approach to optimize the printed circuit boards drill routing process using intelligent water drops," *Comput. Electr. Eng.*, vol. 43, pp. 270–277, Apr. 2015, doi: 10.1016/j.compeleceng.2014.10.005.

[61] T. Letcher and M. Waytashek, "Material property testing of 3D-printed specimen in PLA on an entry-level 3D printer," in *Proc. ASME Int. Mech. Eng. Congr. Expo.*, 2014, pp. 1–14.

[62] A. Alafaghani, A. Qattawi, B. Alrawi, and A. Guzman, "Experimental optimization of fused deposition modelling processing parameters: A design-for-manufacturing approach," *Proc. Manuf.*, vol. 10, pp. 791–803, Jan. 2017, doi: 10.1016/j.promfg.2017.07.079.

[63] V. Kovan, G. Altan, and E. S. Topal, "Effect of layer thickness and print orientation on strength of 3D printed and adhesively bonded single lap joints," *J. Mech. Sci. Technol.*, vol. 31, no. 5, pp. 2197–2201, May 2017, doi: 10.1007/s12206-017-0415-7.

[64] M. K. Agarwala, V. R. Jamalabad, N. A. Langrana, A. Safari, P. J. Whalen, and S. C. Danforth, "Structural quality of parts processed by fused deposition," *Rapid Prototyping J.*, vol. 2, no. 4, pp. 4–19, Dec. 1996, doi: 10.1108/13552549610732034.

[65] R. V. Weeren, M. Agarwala, V. R. Jamalabad, A. Bandyopadhyay, R. Vaidyanathan, N. Langrana, A. Safari, P. Whalen, S. C. Danforth, and C. Ballard, "Quality of parts processed by fused deposition," in *Proc. Int. Solid Freeform Fabr. Symp.*, 1995, pp. 1–12. [Online]. Available: https://repositories.lib.utexas.edu/handle/2152/69339

[66] M. Barletta, A. Gisario, and M. Mehrpouya, "4D printing of shape memory polylactic acid (PLA) components: Investigating the role of the operational parameters in fused deposition modelling (FDM)," *J. Manuf. Processes*, vol. 61, pp. 473–480, Jan. 2021.

[67] S. Khan, K. Joshi, and S. Deshmukh, "A comprehensive review on effect of printing parameters on mechanical properties of FDM printed parts," *Mater. Today, Proc.*, vol. 50, pp. 2119–2127, Jan. 2022.

[68] A. Valerga, M. Batista, J. Salguero, and F. Girot, "Influence of PLA filament conditions on characteristics of FDM parts," *Materials*, vol. 11, no. 8, p. 1322, Jul. 2018.

SINUE ONTIVEROS received the B.S. degree in industrial engineering from the Technological Institute of Los Mochis, Los Mochis, Mexico, in 2003, the M.S. degree in industrial engineering from the Technological Institute of Hermosillo, Hermosillo, Mexico, in 2007, and the Ph.D. degree in industrial engineering from the University of Zaragoza, Zaragoza, Spain, in 2013. Since 2014, he has been a full-time Professor/Researcher with Universidad Autónoma de Baja California, Tecate, Mexico. He is currently an Associate Partner with the Manufacturing Engineering and Advanced Metrology Group, University of Zaragoza. He has authored or coauthored more than 40 articles. His research interests include computed tomography in metrology applications and quality control. He is an active member of the National System of Researchers.

YOLANDA BAEZ-LOPEZ received the B.S. degree in industrial engineering from the Technological Institute of Los Mochis, Mexico, in 2002, and the M.S. degree in industrial engineering and the Doctor of Science degree from the Autonomous University of Baja California (UABC), in 2008 and 2014, respectively. She is currently a Professor in industrial engineering with the Faculty of Engineering, Architecture, and Design, Autonomous University of Baja California. She has been with the Department of Vocational and University linkage coordinator in the Ensenada Campus. She has participated in several research projects on process improvement and the author of more than 50 journal articles, book chapters, and conference papers. Her research interests include six sigma methodology, lean manufacturing, human reliability, and statistical modeling. She is a member of the National System of Researches of the National Council of Science and Technology in Mexico.

JULIÁN ISRAEL AGUILAR-DUQUE received the bachelor's degree in industrial engineering from the Technological Institute of San Luis Potosí (ITSLP), in 2000, the master's degree in industrial engineering from the Technological Institute of Celaya (ITC), in 2008, and the Ph.D. degree in advanced engineering science from the Autonomous University of Ciudad Juárez, in 2021. He has been responsible for multiple projects with financing from UABC and is a collaborator in national and international projects. He is the author or coauthor of 13 articles in indexed international journals, six book chapters, and more than 35 articles in national and international congresses. Regarding human resources training, he has directed two master's and bachelor's theses (he is currently directing two doctoral and one master's). He has the appointment granted by the National System of Level 1 Researcher, until 2025. He was the Leader of the Academic Corps (CA) in the training "Design, Development, and Manufacture of Goods and Services," where he is also a member. His research interests include product design, subtractive and additive manufacturing systems, and process optimization. He has been a Reviewer of Articles of *Indexed Journal*.

JORGE LIMON-ROMERO received the B.S. degree in industrial engineering from the Technological Institute of Los Mochis, Mexico, in 2001, the M.S. degree in industrial engineering from the Technological Institute of Hermosillo, in 2004, and the Doctor of Science degree from the Autonomous University of Baja California, Mexico, in 2013. He is currently a Professor in industrial engineering with the Faculty of Engineering, Architecture, and Design, Autonomous University of Baja California, Mexico. He has participated in several research projects on process improvement and the author/coauthor of more than 40 journal articles, book chapters, and conference operations. His research interests include statistical modeling, multivariate data analysis, and processes and products optimization working with methodologies, such as six sigma and lean manufacturing. He is a member of the National System of Researchers of the National Council of Science and Technology in Mexico and a member of the Optimization of Industrial Processes Network (ROPRIN).